

See discussions, stats, and author profiles for this publication at: <https://www.researchgate.net/publication/257651806>

Bioinspired Hygromorphic Actuator Exhibiting Controlled Locomotion

ARTICLE *in* ACS MACRO LETTERS · OCTOBER 2013

Impact Factor: 5.76 · DOI: 10.1021/mz400439a

CITATIONS

7

READS

62

4 AUTHORS, INCLUDING:



Jacob Prosser

UOP - Honeywell

8 PUBLICATIONS 84 CITATIONS

SEE PROFILE

Bioinspired Hygromorphic Actuator Exhibiting Controlled Locomotion

Sang-Wook Lee,[†] Jacob H. Prosser,[†] Prashant K. Purohit,[‡] and Daeyeon Lee^{*,†}

[†]Department of Chemical and Biomolecular Engineering, and [‡]Department of Mechanical Engineering and Applied Mechanics, University of Pennsylvania, Philadelphia, Pennsylvania 19104, United States

Supporting Information

ABSTRACT: We report a bioinspired hygromorphic double-layered actuator (HDA), of which the movement is controlled by cyclical changes in relative humidity (RH). The basic principle of the HDA lies in the rapid swelling and deswelling of highly hygroscopic layer-by-layer (LbL) assembled films deposited on a moisture-resistant and flexible polytetrafluoroethylene (PTFE) ribbon. We engineer the geometry of the HDA to induce locomotion on a ratchet track. By controlling the exposure time and RH, the HDA is remotely controlled to move a precise number of steps on the ratchet track during one cycle of RH changes. We demonstrate that the step length of the HDA depends on the relative thickness change of the LbL film. We also provide theoretical considerations based on a plate theory and the Flory–Huggins theory to describe the actuation of the HDA. Our work provides fundamental insights into the fabrication and design of hygromorphic actuators driven by RH changes.

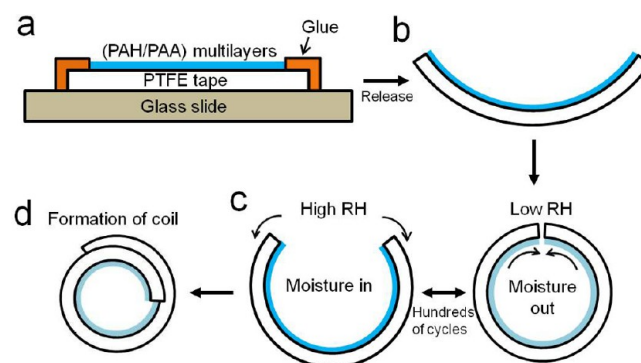


Many plants exhibit actuation in response to changes in environmental conditions such as light, temperature, and humidity.¹ While light- and temperature-responsive movements are mediated through physiological processes in live plants, humidity-induced actuations rely on the differential swelling and deswelling of bonded tissues. Consequently, humidity-induced actuations can occur even if the structure is separated from the maternal plant. For example, after shedding, pine cones change their shape from an open state in dry air to a closed state in humid conditions due to the differential swelling between inner sclerenchyma fibers and outer sclerids.^{2,3} Similarly, seeds from wild wheat are propelled into soil after release by a similar differential expansion mechanism. It has been observed that awns attached to the seed provide direction-dependent force, reversibly bending and unbending under cyclically changing humidity.⁴

Interestingly, many of these natural actuators share a common structural feature in which their humidity-responsive actuation arises from a difference in the elongation length of two different materials (i.e., cells or tissues) interfacially bound to one another to form a laminated, double-layered composite structure. The differential hygroscopic expansion of natural double-layered structures inspires us to fabricate and design synthetic structures that will show actuation in response to changes in humidity. The goal of this work is to develop a bioinspired hygromorphic double-layered actuator (HDA) for which motion can be remotely and precisely controlled by changing the relative humidity (RH) of the local environment and to investigate the effect of the differential expansion of the HDA on their locomotion.

A double-layered structure composed of two layers with different water sorption capacities is fabricated through the layer-by-layer (LbL) deposition of a hygroscopic polyelectrolyte film on one side of a rectangular piece of hydrophobic polytetrafluoroethylene (PTFE) thread tape (Scheme 1a). LbL

Scheme 1. Schematic Diagram Illustrating the Fabrication of a Bioinspired HDA^a



^a(a) PAH/PAA films are deposited on one side of a rectangular strip of PTFE tape using layer-by-layer (LbL) assembly. (b) When the LbL-modified PTFE ribbon is released, it slightly bends. (c) After being repeatedly exposed to high (≥ 80%) and low (≤ 20%) RHs (several hundreds of cycles), (d) it gradually curls into a circular coil.

Received: August 21, 2013

Accepted: October 1, 2013

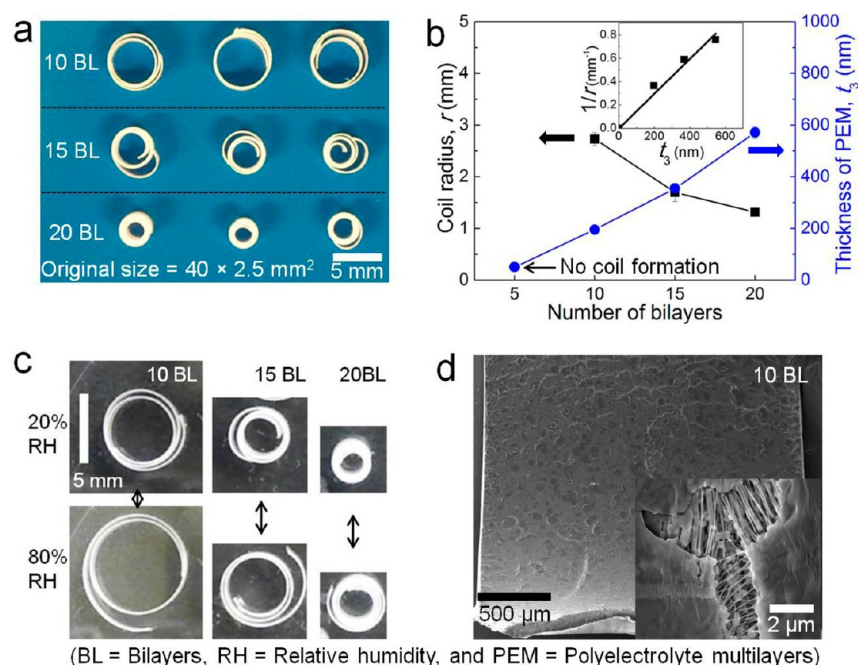


Figure 1. Characteristics of bioinspired hygromorphic double-layered actuators (HDAs). (a) The photograph of HDAs with 10, 15, and 20 bilayers of PAH/PAA LbL films. (b) The radius of coils and the thickness of PAH/PAA LbL films as a function of the number of deposited bilayers. (c) Photographs of HDAs with 10 (left), 15 (middle), and 20 (right) bilayers of PAH/PAA LbL film taken at 20% (top) and 80% RH (bottom). (d) SEM images of a HDA with a 10 bilayer PAH/PAA LbL film. Inset shows cracks in the PAH/PAA LbL film that developed during the coil formation. BL, RH, and PEM denote bilayers, relative humidity, and polyelectrolyte multilayers, respectively.

assembly is a powerful solution-based deposition technique used to fabricate functional nanocomposite thin films with tunable architectures and properties, through alternating adsorption of two different species that interact with each other via electrostatic^{5–8} and/or hydrogen-bonding^{9–12} interactions. Poly(allylamine hydrochloride) (PAH) and poly(acrylic acid) (PAA) are used for LbL assembly of hygroscopic films since the water uptake capacity of PAH/PAA films has been shown to be significant ($\sim 40\%$ of dried film mass at 100% RH).^{13,14} More importantly, these films display rapid humidity-induced swelling/deswelling behaviors, rendering them an ideal choice for the fabrication of hygromorphic actuators (see Supporting Information, Figure S1). Another critical advantage of using PAH/PAA LbL films is that these films can be readily deposited onto nonadhesive surfaces such as PTFE and other hydrophobic polymers.^{11,15,16} Short-range attractions such as van der Waals interactions facilitate the layer-by-layer assembly of PAH/PAA films onto the PTFE sheet.¹⁵ In addition, the morphology of the PTFE tape, which consists of densely packed fibrous structures, enhances the adhesion of the PAH/PAA films onto the substrate, preventing the delamination of the films during repeated cycles of high and low humidity exposure. We note that a double-layered system consisting of a PAH/PAA LbL film and a UV-cured polymer film was recently shown to exhibit actuation under alternating humidity.¹⁶ A novel contribution of our work is that we demonstrate that the locomotion of the actuator can be precisely controlled by changing the time of humidity cycles and the values of relative humidity. These parameters control the swelling of the LbL layers, which ultimately determines the locomotion of the actuator.

When a PAH/PAA LbL film-coated PTFE tape is released from a supporting glass slide, the LbL film-coated PTFE double-layered ribbon spontaneously bends toward the side of

the tape the PAH/PAA LbL film was assembled onto (Scheme 1b). The spontaneous bending occurs because the PAH/PAA LbL film contracts as it dries in ambient air (10–30% RH) after deposition. Interestingly, when these LbL-modified PTFE ribbons are repeatedly exposed to high ($\geq 80\%$) and low ($\leq 20\%$) RHs (Scheme 1c), they gradually curl into circular coils as shown in Scheme 1d. The radius of curvature of these coils eventually reaches a constant value for a given RH after several hundreds of high–low RH cycles. Although we do not completely understand the mechanism behind the gradual change and eventual saturation in the curvature of the released double-layered ribbons, we believe that the swelling properties of the PAH/PAA LbL films evolve slowly under repeated cycles of high and low RHs and reach some steady state. When the swelling and deswelling of the same PAH/PAA LbL film is monitored using quartz crystal microbalance with dissipation (QCM-D) monitoring, the thickness difference between the swollen and deswollen states changes slowly over time and eventually reaches some steady value (see Figure S2, Supporting Information), suggesting some type of structural rearrangement and “aging” in these films. A previous study indeed has shown that LbL films undergo structural changes (i.e., aging) that influence their swelling properties when they are stored in high humidity conditions for an extended period of time.¹⁷

We observe that the radius of these double-layered coils is decreased when the thickness of the deposited PAH/PAA LbL film is increased (Figure 1a,b). To understand the effect of the PAH/PAA film thickness on the curvature of these double-layered coils, the balance of forces and moments in the double-layered composite is accounted for within a plate theory (see Supporting Information for details). We model the PAH/PAA film using the Flory–Huggins theory and the PTFE tape as a linear elastic plate. Assuming that the radius of the LbL-

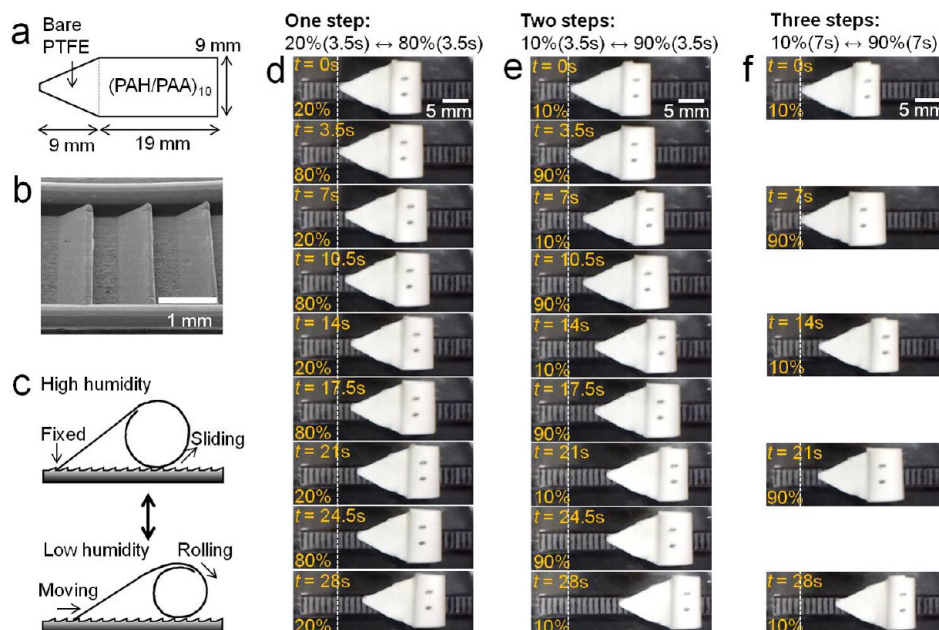


Figure 2. Controlled locomotion of the hygromorphic double-layered actuator (HDA). (a) Design of HDA. The region coated with a PAH/PAA LbL film forms a coiled head of the HDA, whereas the tapered region with bare PTFE forms the tail of the HDA. (b) SEM image of the ratchet track with a step size of ~ 1 mm. (c) Schematic diagrams showing how the HDA moves on the ratchet track. At a high humidity (top), the coiled head slides on the track with its tail anchored on the vertical side of a step in the track. At a low humidity (bottom), the coiled head of the HDA in contact with the track rolls, dragging the tail over the sloped side of the next step on the track. (d–f) Time-lapse photographs showing the controlled locomotion of HDA with one (d), two (e), and three steps (f) during a cycle of low and high RH exposure at 20% and 80% RH for 3.5 s each (d), 10% and 90% RH for 3.5 s each (e), and 10% and 90% RH for 7 s each (f), respectively.

modified PTFE ribbon upon release (Scheme 1b) is linearly proportional to the final radius of the ribbon after multiple cycles of high–low RH exposures (Scheme 1d), the relationship between the coil radius (r) and thickness (t_3) of the PAH/PAA films at a given RH is obtained as follows

$$\frac{1}{r} \sim \frac{\sigma_1 t_3 (h + t_3) (1 - \nu)}{E h^3} \quad (1)$$

where E , h , and ν are the Young's modulus, thickness, and Poisson's ratio of PTFE, respectively, and are nearly constant for all RHs. σ_1 is the principal Cauchy stress in the PAH/PAA film in the lateral direction, which is dependent on RH. Note that σ_1 is the same in any direction in the plane of the film because it is isotropic (i.e., PTFE tape is subject to equibiaxial stretching). Since the thickness of the PTFE tape ($h \sim 100 \mu\text{m}$) is much larger than the thickness of PAH/PAA films ($h \gg t_3$) and σ_1 depends on the ambient RH, eq 1 reduces to $1/r \propto t_3$ for a given RH (see Figure S4, Supporting Information). This relationship is in good agreement with the experimental result as shown in Figure 1b.

One of the fascinating aspects of these double-layered coils is their actuating capability in response to changes in RH. For example, swelling and deswelling (between 80% and 20% RH) of the PAH/PAA LbL films reversibly induce partial uncoiling and coiling of these hygromorphic double-layered actuators (HDAs), respectively (Figure 1c). This reversible actuation occurs despite the fact that cracks develop in the PAH/PAA LbL films during coiling upon release from the supporting glass slides. Crack formation in the LbL films is likely due to the glassy nature of these films under dry conditions (Figure 1d and inset).¹⁴ Nevertheless, the adhesion between PAH/PAA LbL films and the PTFE substrate is strong enough to prevent delamination of the LbL films during repeated swelling and

deswelling cycles (inset in Figure 1d). No further development of cracks is observed even after 3600 cycles (10 h) of alternating exposures between 20% and 80% RH for 5 s each (see Supporting Information, Figure S3). We believe these cracks form to relieve the stress that develops in the LbL film during aging (i.e., molecular reorganization that takes place under repeated cycles of high and low humidity exposure).

We engineer the shape of a hygromorphic double-layered actuator (HDA) to induce unidirectional locomotion on a ratchet track in response to cyclical changes in relative humidity (RH). The design for the locomotive HDA is illustrated in Figure 2. A piece of rectangular PTFE tape is cut into a shape consisting of a rectangular region with a triangular taper on one end as shown in Figure 2a. The rectangular region of the PTFE ribbon is coated with 10 bilayers (BL) of a PAH/PAA film (equivalent to 190 nm in thickness on a silicon wafer) and subsequently subjected to several hundred cycles of high ($\geq 80\%$) and low ($\leq 20\%$) RH exposures to form the coiled head of the HDA. The tapered region with bare PTFE forms the tail of the HDA. In analogy to awns attached to seeds of wild wheat that have epidermal hairs tilted in one direction to enable propelling of seeds into the ground in a ratchet manner,⁴ a ratchet track having asymmetrically sloped steps is used to facilitate the unidirectional locomotion of the HDA (Figure 2b). At high humidity, the radius of the coiled head increases (i.e., the uncurling of the coiled head occurs) due to the swelling of the PAH/PAA film; the center-of-mass of the HDA moves forward (head direction) due to the anchoring of the tip of its tail on the vertical side of a ratchet step and the sliding of the head forward on the track (top in Figure 2c). Upon reduction of the humidity, the radius of the head becomes smaller in such a way that the head recoils and rolls on the track; this motion drags the tail forward and subsequently

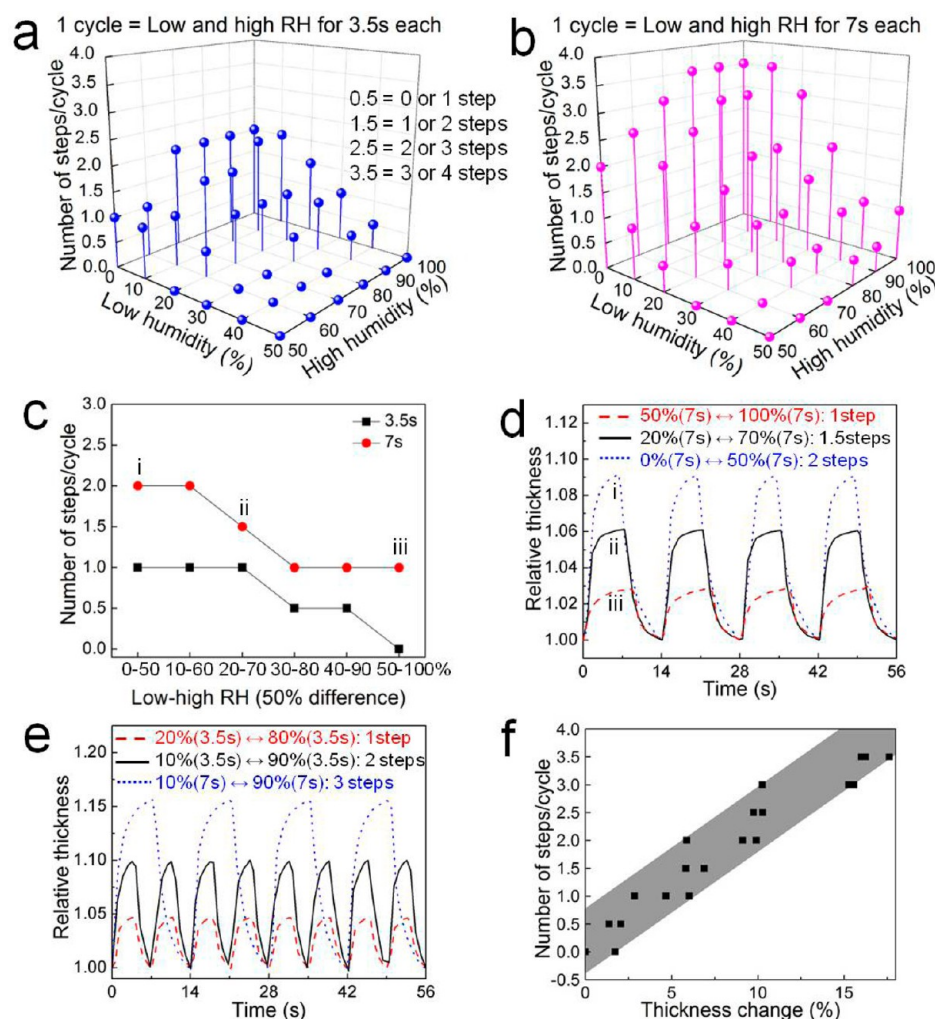


Figure 3. Relationship between the step length of the HDA and the relative thickness change of the PAH/PAA LbL film. (a,b) Step length of the HDA measured by the number of steps on the track during a single cycle of low and high RH exposures. 36 RH combinations are used, and the exposure time at each humidity is 3.5 s (a) or 7 s (b). (c) Step length of the HDA measured at six humidity combinations with a 50% RH difference between high and low RHs. (d) Relative thickness change of the PAH/PAA films measured by a QCM-D for three cases in (c) (labels i, ii, and iii) where the number of steps are 2, 1.5, and 1, respectively. (e) Relative thickness change of PAH/PAA films in three cases in which the step lengths of the HDA are 1, 2, and 3 steps on the track as shown in Figure 2d–f, respectively. (f) Step length of HDA as a function of thickness change of PAH/PAA films.

moves the center-of-mass of the HDA forward (bottom in Figure 2c).

On the basis of this bioinspired ratchet mechanism, the locomotion of the HDA is precisely tuned by controlling RH and RH cycle time, both of which affect the extent of swelling/deswelling of the PAH/PAA LbL films. Note that the step length of the locomotive HDA is measured by counting the number of steps on the ratchet track on which the HDA travels during a single cycle of low and high RH exposures. We first demonstrate that the HDA can travel one step at a time on the track during a cycle between 20% and 80% RH with 3.5 s exposure time at each RH (Figure 2d and see Movie S1 (mz400439a_si_002.avi), Supporting Information). The step length of the HDA can be increased to two steps on the track by cyclically exposing the HDA to 10% and 90% RH, using the same exposure time (3.5 s each) (Figure 2e and see Movie S2 (mz400439a_si_003.avi), Supporting Information). Step length of the HDA is further increased to three steps on the track by simply increasing the exposure time (7 s each) at the same RH

combination of 10% and 90% RH (Figure 2f and see Movie S3 (mz400439a_si_004.avi), Supporting Information).

Careful examination of the influence that RH and exposure time have on step length reveals that neither the difference between low and high RH nor the RH exposure time solely determines the step length of the HDA. In general, the larger the difference between low and high RHs (Δ RH) and the longer the exposure time is, the larger the step length of the HDA is, as shown in Figure 3a, b. Figure 3c also shows that the step length of the HDA decreases as the absolute values of RHs increase, even though all RH combinations have the same difference (Δ RH = 50%) between high and low RHs. In addition, increasing the exposure time from 3.5 to 7 s does not double the step length for 20–70 and 50–100% RH combinations (Figure 3c). Therefore, it appears that the RH difference and exposure time have an interdependent effect on the HDA step size. To find a dominant parameter that determines the step length, a reduction of dimensionality between the RH difference and exposure time is considered.

To reduce these two independent variables into a single determinable parameter that significantly influences the step length of the HDA, we revisit eq 1 and focus on the volume change of the PAH/PAA films with varying RH and exposure time. By modeling the (de)swelling of the PAH/PAA films using an analogy to the kinetics of the (dis)charging of capacitors (for details, see Supporting Information), the volume of the PAH/PAA films upon cycling between low and high RHs is obtained as a function of time (see Figure S5, Supporting Information). The characteristic time constants for the swelling and deswelling of the PAH/PAA LbL films when RH is changed from 20% to 80% and from 80% to 20% (Figure S1, Supporting Information) are $\tau_s = 2.8$ s and $\tau_d = 8.0$ s, respectively. These humidity- and time-dependent volume changes (in Figure S5, Supporting Information) are used to obtain the corresponding changes in the thickness (t_3), stress (σ_1) (see Supporting Information), and, subsequently, the radius of the coiled head (r) using eq 1. We note that r is geometrically related to the step length on the ratchet (see Figure S6, Supporting Information). On the basis of the relationship between r and the step length, the step length of the HDA is calculated as a function of the thickness change (Δt_3) of the PAH/PAA films during a single cycle of low and high RH exposures and is found to have a more or less linear relationship, especially when the thickness change is small (<10%) (see Figure S7, Supporting Information). This theoretical consideration illustrates that the mechanism behind the increase of r at high RH is mainly a reduction in σ_1 , which overcompensates the increase of t_3 in eq 1 (see Figure S8, Supporting Information).

To validate these theoretical considerations, we measure the real-time thickness change of the PAH/PAA LbL film upon cycling between low and high RHs using a quartz crystal microbalance with dissipation (QCM-D) monitoring. Figure 3d shows that the relative thickness changes of PAH/PAA films under 0–50%, 20–70%, and 50–100% RH combinations (labels i, ii, and iii in Figure 3c, respectively) monotonically decrease, showing a seemingly linear correlation to the step length in each case (i.e., 2, 1.5, and 1 steps, respectively). Moreover, the relative thickness change of PAH/PAA LbL films that induces the locomotive HDA to move one, two, and three steps at a time on the ratchet track (Figure 2d–f) appears to be linearly correlated with the step length (Figure 3e). When we plot the step length of the HDA as a function of the thickness change of PAH/PAA films, it can be seen that the step length of the HDA is approximately linearly proportional to the thickness change (Δt_3) of the PAH/PAA films, showing qualitative agreement with our theoretical considerations (Figure 3f).

In summary, we have demonstrated bioinspired hygro-morphic double-layered actuators (HDAs) that exhibit locomotion. We have shown that the geometry of the HDA can be controlled simply by varying the thickness of the hygroscopic layer-by-layer (LbL) films that are deposited on hydrophobic PTFE. The locomotion of the HDAs on a ratchet track is remotely and precisely tuned by controlling the relative humidity (RH) and exposure time. The relative thickness change of the hygroscopic LbL films is experimentally and theoretically found to be more or less linearly correlated with the step length of the locomotive HDA during a single cycle of low and high RH exposures. On the basis of the simplicity and the controllability of our approach, we expect that the present work can be further expanded for fabricating and designing a wide range of miniaturized devices capable of cargo trans-

portation,¹⁶ energy conversion,¹⁸ and humidity sensing (which we already have demonstrated as shown in Figure S9, Supporting Information). In addition, by combining with the patternability of layer-by-layer films using various lithographic techniques,¹⁰ it will be possible to control the microscale geometry of HDAs to induce more complex actuations in response to water.¹⁹ Furthermore, the fabrication of actuators with light-, electro-, and thermo-responsive polymers^{20–22} as well as hydrogels responsive to the surrounding medium^{23,24} will extend the applicability of these actuators into tunable optics, tissue engineering, and soft robotics.

■ ASSOCIATED CONTENT

Supporting Information

Experimental section, thickness change of a PAH/PAA film during swelling and deswelling, SEM images of cracks in PAH/PAA LbL films, humidity detector using a hygro-morphic double-layered actuator, and theoretical work. This material is available free of charge via the Internet at <http://pubs.acs.org>.

■ AUTHOR INFORMATION

Corresponding Author

*E-mail: daeyeon@seas.upenn.edu.

Notes

The authors declare no competing financial interest.

■ ACKNOWLEDGMENTS

This work was supported primarily by a NSF CAREER Award (DMR-1055594) and partly by the PENN MRSEC (DMR-1120901). PKP acknowledges partial support through an NSF grant number NSF CMMI-1066787.

■ REFERENCES

- (1) Burgert, I.; Fratzl, P. *Philos. Trans. R. Soc. A: Math. Phys. Eng. Sci.* **2009**, *367*, 1541–1557.
- (2) Dawson, J.; Vincent, J. F. V.; Rocca, A. M. *Nature* **1997**, *390*, 668–668.
- (3) Reyssat, E.; Mahadevan, L. *J. R. Soc. Interface* **2009**, *6*, 951–957.
- (4) Elbaum, R.; Zaltzman, L.; Burgert, I.; Fratzl, P. *Science* **2007**, *316*, 884–886.
- (5) Decher, G.; Schlenoff, J. B. *Multilayer thin films: sequential assembly of nanocomposite materials*, 1st ed.; Wiley-VCH: Weinheim, 2003.
- (6) Shiratori, S. S.; Rubner, M. F. *Macromolecules* **2000**, *33*, 4213–4219.
- (7) Decher, G.; Eckle, M.; Schmitt, J.; Struth, B. *Curr. Opin. Colloid Interface Sci.* **1998**, *3*, 32–39.
- (8) Lvov, Y.; Ariga, K.; Ichinose, I.; Kunitake, T. *J. Am. Chem. Soc.* **1995**, *117*, 6117–6123.
- (9) Sukhishvili, S. A.; Granick, S. *J. Am. Chem. Soc.* **2000**, *122*, 9550–9551.
- (10) Yang, S. Y.; Rubner, M. F. *J. Am. Chem. Soc.* **2002**, *124*, 2100–2101.
- (11) Lutkenhaus, J. L.; Hrabak, K. D.; McEnnis, K.; Hammond, P. T. *J. Am. Chem. Soc.* **2005**, *127*, 17228–17234.
- (12) Kharlampieva, E.; Kozlovskaya, V.; Sukhishvili, S. A. *Adv. Mater.* **2009**, *21*, 3053–3065.
- (13) Secrist, K. E.; Nolte, A. J. *Macromolecules* **2011**, *44*, 2859–2865.
- (14) Lee, S.-W.; Lee, D. *Macromolecules* **2013**, *46*, 2793–2799.
- (15) Park, J.; Hammond, P. T. *Macromolecules* **2005**, *38*, 10542–10550.
- (16) Ma, Y.; Zhang, Y. Y.; Wu, B. S.; Sun, W. P.; Li, Z. G.; Sun, J. Q. *Angew. Chem., Int. Ed.* **2011**, *50*, 6254–6257.
- (17) Itano, K.; Choi, J. Y.; Rubner, M. F. *Macromolecules* **2005**, *38*, 3450–3460.

- (18) Ma, M. M.; Guo, L.; Anderson, D. G.; Langer, R. *Science* **2013**, 339, 186–189.
- (19) Byun, M.; Santangelo, C. D.; Hayward, R. C. *Soft Matter* **2013**, DOI: 10.1039/c3sm50627d.
- (20) Kim, J.; Hanna, J. A.; Byun, M.; Santangelo, C. D.; Hayward, R. C. *Science* **2012**, 335, 1201–1205.
- (21) Wang, E.; Desai, M. S.; Lee, S.-W. *Nano Lett.* **2013**, 13, 2826–2830.
- (22) Morales, D.; Palleau, E.; Dickey, M. D.; Velez, O. D. *Soft Matter* **2013**, DOI: 10.1039/C3SM51921J.
- (23) Palleau, E.; Morales, D.; Dickey, M. D.; Velez, O. D. *Nat. Commun.* **2013**, 4, 2257.
- (24) Therien-Aubin, H.; Wu, Z. L.; Nie, Z. H.; Kumacheva, E. *J. Am. Chem. Soc.* **2013**, 135, 4834–4839.